AIAA JOURNAL
Vol. 36, No. 1, January 1998

Direct Coupled Load Verification of Modified Structural Component

Y. Yasui*
Nippon Telegraph and Telephone Corporation, Yokosuka, Kanagawa 239, Japan

An analytical verification method for structural dynamics subject to partial design change is proposed. The method can predict time-domain structural dynamic responses after the changes are implemented, incorporated with the entire structural characteristics including the unchanged portion, by using small numbers of modal parameters of the original structure and the modified component. The concise computation of the degrees of freedom of the modal representation, which are formulated to retain the residual flexibility in the equation of motion, can correctly provide changed effects. The representation of the component mode synthesis and the force equilibrium between the changed component and the main structure are utilized to develop the algorithm, which yields the modal mass-stiffness conversion in the component modes. Applying this method to the spacecraft redesign, without the physical property information of the launch vehicle or repetition of coupled load analysis, the established algorithm can improve the prediction of the coupled spacecraft and launch vehicle structural dynamics. A reanalysis can be implemented using a limited number of available modal parameters from the coupled analysis for the original structure. Demonstrations applied to simple beam and spacecraft–launch vehicle models presented show the effectiveness of the method.

Nomenclature

C = damping matrix of entire structure
F = external force
f_l = modal force, i.e., $[\phi_l]^T\{F\}$
I = identity matrix
K = stiffness matrix of entire structure
M = mass matrix of entire structure
M_{bi} = mass matrix coupling part between component modal and boundary degree of freedom (DOF) $(b \times i)$
Q_j = modal DOF of entire structure
q_i = modal DOF of component
s = Laplacian operator
ΔC = change of damping matrix
ΔK = change of stiffness matrix
ΔM = change of mass matrix
ζ = diagonal coefficient matrix defined in Eq. (25)
η_i = transformed DOF defined in Eq. (28)
ϕ_j = mode shape of original entire structure

Subscripts

a = DOF of component subject to design change
b = boundary DOF between component and main structure
e = DOF of main structure including driving points by external force
i = modal DOF of component
j = modal DOF of entire structure
v = DOF of main structure and boundary
o = component interior grid points

Superscripts

T = transpose of matrix
-1 = inverse of matrix

Introduction

BECAUSE of the competitive market, current spacecraft development demands quick fabrication and low cost. While providing a low cost, vendors must design optimal spacecraft satisfying various payload performances as required by customers and must produce their spacecraft in a timely fashion. However, original spacecraft design and analysis procedures are time consuming and costly. One solution to these problems is to develop a flexible reanalysis methodology that allows design changes from the prototype structure at arbitrary time and manner. This will help circumvent interruptions in development and repeating series of analyses and tests as a result of the design changes. Note that the spacecraft structure is exposed to critical vibration and acoustic conditions as part of launch vehicle structure at launch.[1] Reanalyzing the structural load coupled with the launch vehicle, i.e., coupled load analysis (CLA), is indispensable when major spacecraft structural characteristics are changed. In general, the analytical model of a launch vehicle is not available for the spacecraft designer or it is difficult to conduct the coupled analysis. This is probable for general component design analysis. CLA is implemented by the launch vehicle vendor, although the design is changed at the spacecraft. Repetition of CLA is prohibitive in terms of time and cost. Therefore, a convenient and reliable reanalysis technique is desired to alleviate redesign.

Many methods can be applied to the coupled load reanalysis. The perturbation-type technique has been proposed and improved[2–4]; however, it still has a problem in its ability to handle large changes. The method using predictor-corrector iteration[5] may alleviate this limitation. However, the truncation effect of modal representation has not been examined. Also, the method based on the sensitivity analysis[6] can only provide reference to the effect of the change on individual parameters and is not convenient for direct verification. In general, CLA is implemented using modal degree of freedom (DOF). Also, the spacecraft is formulated by the component mode synthesis (CMS) in CLA. The formulation in CMS can provide attractive insights for the reanalysis using modal DOF. A survey of CMS prominent methods is found in Ref. 7. CMS can provide accurate prediction for spacecraft-launch vehicle coupled load response.[8,9] Off-the-shelf software packages including CMS coding[10] have been developed and are being used without basic knowledge of the method. After application to real design activities and related structural dynamics problems,[11] the advantages and limitations of the method have been examined.[12,13]

In employing modal DOF, the accuracy of reanalysis is also driven by the number of employed modes. This leads to the mode truncation problem as commonly found in modal methods using modal DOF. The CMS equations are intentionally formulated to suppress the error induced by mode truncation. The ideas of residual flexibility, attachment modes, or constraint modes of the Craig–Bampton

Received March 20, 1997; revision received Aug. 20, 1997; accepted for publication Aug. 21, 1997.

*Senior Research Engineer, Spacecraft Structure Specialist, NTT Wireless Systems Laboratories, 1-1 Hikarinooka. Member AIAA.

formulation are derived from the research of the CMS striving against mode truncation error.

In general, the modes employed in coupled analysis are also truncated. The truncation effect in the component is suppressed by the formulation of the CMS. However, the effect raised by the interaction between the unretained modes of the coupled structure, i.e., global modes, and changed component parameters causes certain error. An equation formulation and procedure must be developed that can compensate for the mode truncation error in the coupled load calculation. A frequency-domain method has been proposed[14] to handle this problem. However, the time-domain method using CLA results is more convenient for application to the spacecraft design procedure than the frequency-domain method. Focusing on the mode truncation effect, the time response in reanalysis is improved by the algorithm based on the CMS formulation and the force equilibrium between the changed component and entire structure. The formulation is derived from the idea of the residual flexibility and mode acceleration method.[2] The form of the proposed method is amenable to numerical computation with standard finite element analysis techniques. This method can be used for a general time-domain reanalysis using modal DOF and is demonstrated with a sample beam model and a spacecraft-launch vehicle CLA application using typical parameters.

Modal Formulation of a Modified Structure

The basic equation of the coupled dynamics of the entire structure with the component (spacecraft) and the main structure (launch vehicle) is defined as

$$[M]s^2\{u\} + [C]s\{u\} + [K]\{u\} = \{F\} \tag{1}$$

When using modal DOF, Eq. (1) becomes

$$[m_j]s^2\{Q_j\} + [c_j]s\{Q_j\} + [k_j]\{Q_j\} = [\phi_j]^T\{F\} \tag{2}$$

where

$$\{u\} = [\phi_j]\{Q_j\} \tag{3}$$

and $[m_j]$, $[c_j]$, and $[k_j]$ are diagonal matrices of modal mass, damping, and stiffness of the entire structure. The applied force induced by launch vehicle thrust and external environmental forces is identical, even though the spacecraft design is changed. This means the right-hand side of Eq. (1) is unchanged before and after a design change is implemented. Because the launch vehicle is heavy and large enough in applications to the CLA with spacecraft, it is assumed that the mode shape at the point where the external force is applied is unchanged by the spacecraft design change. In this sense, the right-hand side of Eq. (2) also remains unchanged before and after the design change.

The structural component is defined with modal DOF and physical DOF at the boundary according to the representation of the CMS in Ref. 9. Using fixed boundary component normal modes Φ and constraint modes G, the structural component is transformed into component modal representation:

$$\begin{Bmatrix} u_0 \\ \hdashline u_b \end{Bmatrix} = \left[\begin{array}{c:c} \Phi & G \\ \hdashline 0 & I \end{array}\right] \begin{Bmatrix} q_i \\ \hdashline u_b \end{Bmatrix} \tag{4}$$

With the component representation obtained by the linear transformation of Eq. (4), the force equilibrium equation for a component may be written as

$$\left[\begin{array}{c:c} m_i & M_{ib} \\ \hdashline M_{ib}^T & M_{bb} \end{array}\right] s^2 \begin{Bmatrix} q_i \\ \hdashline u_b \end{Bmatrix} + \left[\begin{array}{c:c} c_i & 0 \\ \hdashline 0 & 0 \end{array}\right] s \begin{Bmatrix} q_i \\ \hdashline u_b \end{Bmatrix} + \left[\begin{array}{c:c} k_i & 0 \\ \hdashline 0 & k_{bb} \end{array}\right] \begin{Bmatrix} q_i \\ \hdashline u_b \end{Bmatrix} = \begin{Bmatrix} 0 \\ \hdashline F_b \end{Bmatrix} \tag{5}$$

where $[m_i]$, $[c_i]$, and $[k_i]$ are diagonal matrices. The component is driven by the time-varying force F_b at boundary points b. Using Eq. (5) as the representation for the component portion, Eq. (1) can be rewritten as

$$\left[\begin{array}{c:c:c} m_i & M_{ib} & 0 \\ \hdashline M_{ib}^T & \bar{M}_{bb} & M_{be} \\ \hdashline 0 & M_{be}^T & M_{ee} \end{array}\right] s^2 \begin{Bmatrix} q_i \\ \hdashline u_b \\ \hdashline u_e \end{Bmatrix} + \left[\begin{array}{c:c:c} c_i & 0 & 0 \\ \hdashline 0 & \bar{C}_{bb} & 0 \\ \hdashline 0 & 0 & C_{ee} \end{array}\right] s \begin{Bmatrix} q_i \\ \hdashline u_b \\ \hdashline u_e \end{Bmatrix} + \left[\begin{array}{c:c:c} k_i & 0 & 0 \\ \hdashline 0 & \bar{K}_{bb} & K_{be} \\ \hdashline 0 & K_{be}^T & K_{ee} \end{array}\right] \begin{Bmatrix} q_i \\ \hdashline u_b \\ \hdashline u_e \end{Bmatrix} = \begin{Bmatrix} 0 \\ \hdashline 0 \\ \hdashline F_e \end{Bmatrix} \tag{6}$$

The boundary physical matrices $\bar{M}_{bb}$, $\bar{C}_{bb}$, and $\bar{K}_{bb}$ contain the properties of both the component and the main structure. The displacement of the system equation in Eq. (6) can be represented with modal DOF as Eq. (2) by the following linear transformation:

$$\begin{Bmatrix} q_i \\ \hdashline u_b \\ \hdashline u_e \end{Bmatrix} = [\phi_j]\{Q_j\} \tag{7}$$

Reanalysis in Modal Representation

To avoid unnecessary calculation in the large data space of DOF including negligibly small responses induced by the high-frequency modes, fewer modal DOFs are used than physical DOFs. However, if the design is changed, it may produce a significant error as a result of the interaction between unretained modes and the change in property, because the change violates the orthogonality of the modes. The design change alters the mode shape defined as an eigencharacteristic into an arbitrary assumed deflection for a linear transformation. Therefore, the higher modes of the original structure cannot be ignored simply because their resonant frequencies are much higher than that required for verification.

Assuming the design change occurred after the first CLA, the modal response and mode shape parameters of the original structure have already been obtained. Thus, if the response after the change can be represented by the modal DOF of the original structure, extracting a new eigenvalue or mode shape coupled with all of the DOF is not required.

Mode Truncation and Residual Flexibility

The problem is the effect of the truncated modes, even though the equation formulation of modal DOF is concise and convenient. It has been proven that the problem of mode truncation is improved by introducing residual flexibility[12] into the equation of motion or by employing the mode acceleration method.[13] These two methods are developed from basically similar ideas. However, both require inversion of the stiffness matrix of the entire structure. Therefore, in a straightforward approach, the stiffness or flexibility matrix of the unchanged portion is required.

The equation of the entire structure after changes, including residual flexibility, is presented in Ref. 15, i.e.,

$$\left[\begin{array}{c:c} m_j & 0 \\ \hdashline 0 & \Delta M \end{array}\right] s^2 \begin{Bmatrix} Q_j \\ \hdashline u_a \end{Bmatrix} + \left[\begin{array}{c:c} c_j & 0 \\ \hdashline 0 & \Delta C \end{array}\right] s \begin{Bmatrix} Q_j \\ \hdashline u_a \end{Bmatrix} + \left[\begin{array}{c:c} k_j + \phi_j^T Z \phi_j & -\phi_j^T Z \\ \hdashline -Z\phi_j & Z + \Delta K \end{array}\right] \begin{Bmatrix} Q_j \\ \hdashline u_a \end{Bmatrix} = \begin{Bmatrix} f_j \\ \hdashline 0 \end{Bmatrix} \tag{8}$$

where the second row comprises the changed component properties and residual stiffness matrix Z, i.e., the inverse of the residual flexibility matrix. In the spacecraft design change, the residual stiffness matrix Z is derived from the entire structural characteristics including the launch vehicle. In general, this matrix will not actually be available for spacecraft designers.

The proposed idea of this paper can be explained from Eq. (8) and the mode acceleration method. As truncation compensation, the displacement u can be expressed as the linear combination of modal displacements and an additional quasistatic response for truncation error compensation:

$$\{u\} = [\phi_j]\{Q_j\} + \{u_h\} \tag{9}$$

where $\{u_h\}$ is the vector to compensate for truncated high-frequency modes. Then, similar to the idea of CMS, the effects of the inertia and the damping of the high-frequency modes are assumed to be negligible for the total force equilibrium equation. This leads to

$$s^2\{u_h\} \cong s\{u_h\} \cong 0 \tag{10}$$

Premultiplying mode shape ϕ_j^T to the second row of Eq. (8), it is substituted into the first row of Eq. (8) to eliminate the residual stiffness Z. Equations (9) are applied to u_a in Eq. (8), and Eq. (10) is also introduced into Eq. (8), which becomes

$$\left[m_j + \phi_j^T \Delta M \phi_j\right] s^2\{Q_j\} + \left[c_j + \phi_j^T \Delta C \phi_j\right] s\{Q_j\} + \left[k_j + \phi_j^T \Delta K \phi_j\right]\{Q_j\} + \left[\phi_j^T \Delta K\right]\{u_h\} = \{f_j\} \tag{11}$$

As a comparison, the perturbation approach[2–4] is applied to the system equation. This is represented by the mode projection, i.e.,

$$\left[m_j + \phi_j^T \Delta M \phi_j\right] s^2\{Q_j\} + \left[c_j + \phi_j^T \Delta C \phi_j\right] s\{Q_j] + \left[k_j + \phi_j^T \Delta K \phi_j\right]\{Q_j\} = \{f_j\} \tag{12}$$

This is the standard modal method with a truncated set of modes, ignoring the effect of the high-frequency mode. Comparing Eqs. (11) and (12), the only difference is the fourth term of the left-hand side of Eq. (11). This implies that the residual flexibility effect for changed matrix in Eq. (8) can be interpreted as an additional term in the mode projection representation with retained modes, that is, the interaction between the change of stiffness and compensation vector representing higher-frequency mode deflections.

Truncation Compensation with Mode Acceleration

The mode acceleration technique is expressed as

$$\{u\} = [K]^{-1}\left\{F - M\phi_j s^2 Q_j - C\phi_j s Q_j\right\} \tag{13}$$

The fundamental idea of the mode acceleration technique is to modify static displacement using force equilibrium between strain force via the physical stiffness matrix and the combination of inertia and damping force derived from the response of the modal DOF and external force. Using Eq. (9) in Eq. (13), we obtain

$$\{u_h\} = [K]^{-1}\left\{F - M\phi_j s^2 Q_j - C\phi_j s Q_j\right\} - [\phi_j]\{Q_j\} \tag{14}$$

This can be rewritten as

$$\{u_h\} = [K]^{-1}\left\{F - M\phi_j s^2 Q_j - C\phi_j s Q_j - K\phi_j Q_j\right\} \tag{15}$$

Introducing Eq. (15) into the last term on the left-hand side of Eq. (11), the last term becomes

$$[\phi_j]^T[\Delta K]\{u_h\} = [\phi_j]^T[\Delta K][K + \Delta K]^{-1}\left\{F - M\phi_j s^2 Q_j - C\phi_j s Q_j - (K + \Delta K)\phi_j Q_j\right\} \tag{16}$$

It can be deduced that to obtain the truncation compensation term of the left-hand side of Eq. (16) the inversion of the entire stiffness matrix is required. When this approach is applied to the component mode representation of Eq. (5), we can use the advantage of the form of the stiffness matrix in Eq. (6). As shown in Eq. (6), the inverse of the stiffness matrix can be processed at the two submatrices as given by

$$K^{-1} = \left[\begin{array}{c|c} k_i^{-1} & 0 \\ \hline 0 & K_{vv}^{-1} \end{array}\right] \tag{17}$$

where

$$K_{vv} = \left[\begin{array}{c|c} \bar{K}_{bb} & K_{be} \\ \hline K_{eb} & K_{ee} \end{array}\right] \tag{18}$$

The inverse of the stiffness matrix will be obtained partially even though the total stiffness is unknown. Hence, ignoring the second and third rows of the matrix in Eq. (6) denoted with the subscripts of b and e, i.e., the launch vehicle and the boundary area, we proceed to calculate the upper submatrix.

The partition between the upper and lower matrices is defined as

$$M = \left[\begin{array}{c} M_a \\ \hline M_v \end{array}\right], \qquad K = \left[\begin{array}{c} K_a \\ \hline K_v \end{array}\right], \qquad C = \left[\begin{array}{c} C_a \\ \hline C_v \end{array}\right] \tag{19}$$

The change in the component is transformed into the changes of the component modes and physical property at the boundary DOF in the representation of CMS. Assuming that error compensation is performed for the component modes, we deal with the changes confined in the component modes first. The change effect of the boundary portion is discussed later. Assuming that change is within component modes, the upper and lower partition of the changed stiffness matrix is

$$\Delta K = \left[\begin{array}{c} \Delta K_a \\ \hline 0 \end{array}\right] = \left[\begin{array}{c} \Delta k_i \\ \hline 0 \end{array}\right] \tag{20}$$

Then, the right-hand side of Eq. (16) is transformed by the component stiffness matrix representation in Eq. (17). Equation (16) becomes

$$\begin{aligned}[\phi_j]^T[\Delta K][K + \Delta K]^{-1} &\times \left\{F - M\phi_j s^2 Q_j - C\phi_j s Q_j - (K + \Delta K)\phi_j Q_j\right\} \\ &= [\phi_j]^T \left[\begin{array}{c|c} \Delta k_i & 0 \\ \hline 0 & 0 \end{array}\right]\left[\begin{array}{c|c} (k_i + \Delta k_i)^{-1} & 0 \\ \hline 0 & K_{vv}^{-1} \end{array}\right] \\ &\times \left\{\begin{array}{c} F_a - M_a\phi_j s^2 Q_j - C_a\phi_j s Q_j - [k_i + \Delta k_i]\phi_j Q_j \\ \hline F_v - M_v\phi_j s^2 Q_j - C_v\phi_j s Q_j - [K_v]\phi_j Q_j \end{array}\right\}\end{aligned} \tag{21}$$

The matrix multiplication of the right-hand side is executed. Then, Eq. (21) is rewritten as

$$\begin{aligned}[\phi_j]^T[\Delta K][K + \Delta K]^{-1} &\times \left\{F - M\phi_j s^2 Q_j - C\phi_j s Q_j - (K + \Delta K)\phi_j Q_j\right\} \\ &= [\phi_j]^T \left\{\begin{array}{c} \zeta F_a - \zeta\left[M\phi_j s^2 Q_j - C\phi_j s Q_j\right] - \zeta[k_i + \Delta k_i]\phi_j Q_j \\ \hline 0 \end{array}\right\}\end{aligned} \tag{22}$$

where ζ is a diagonal matrix that represents each generalized stiffness change, which is defined as

$$[\zeta] = [\Delta k_i][k_i + \Delta k_i]^{-1} \tag{23}$$

Then, the last term in Eq. (11) yields

$$\begin{aligned}[\phi_j]^T[\Delta K]\{u_h\} &= [\phi_j]^T \\ &\times \left\{\begin{array}{c} \zeta F_a - \zeta\left[M_a\phi_j s^2 Q_j - C_a\phi_j s Q_j\right] - \zeta[k_i + \Delta k_i]\phi_j Q_j \\ \hline 0 \end{array}\right\}\end{aligned} \tag{24}$$

The external force F_a does not exist for the component.

To simplify the explanation, the damping matrix is eliminated in the equation, which can be treated as the same manner as the mass matrix because it is the same expression of term, if the damping matrix on the physical DOF is available. Equation (21) can be further simplified as

$$[\phi_j]^T[\Delta K]\{u_h\} = [\phi_j]^T \left\{\begin{array}{c} -\zeta\left[M_a\phi_j s^2 Q_j\right] - \zeta[k_i + \Delta k_i]\phi_j Q_j \\ \hline 0 \end{array}\right\} \tag{25}$$

It is noted that the right-hand term of Eq. (25) implies projection by the global mode ϕ_j. Premultiplication of the right-hand side of

Eq. (25) is represented by the deployed matrix and vector multiplication expression as

$$[\phi_j]^T[\Delta K]\{u_h\} = -[\phi_j]^T\left[\begin{array}{c}\zeta M_a\\ \hline 0\end{array}\right][\phi_j]s^2\{Q_j\} - \left[\begin{array}{c}\zeta[k_i+\Delta k_i]\\ \hline 0\end{array}\right][\phi_j]\{Q_j\} \tag{26}$$

Hence, introducing Eq. (26) into Eq. (11), the equation of motion yields a modified formulation of the projection by the original global modes of the entire structure. Considering the form of Eq. (26), because the change is introduced only to the upper submatrix, i.e., the component mode portion in the total equation of motion of Eq. (11), the truncation compensation term of Eq. (26) is introduced into the component representation in Eq. (5):

$$\left[\begin{array}{c|c} m_i & M_{ib}\\ \hline M_{ib}^T & M_{bb}\end{array}\right]s^2\left\{\begin{array}{c} q_i\\ \hline u_b\end{array}\right\} + \left[\begin{array}{c|c} k_i+\Delta k_i & 0\\ \hline 0 & K_{bb}\end{array}\right]\left\{\begin{array}{c} q_i\\ \hline u_b\end{array}\right\} - \left[\begin{array}{c|c} \zeta m_i & \zeta M_{ib}\\ \hline 0 & 0\end{array}\right]s^2\left\{\begin{array}{c} q_i\\ \hline u_b\end{array}\right\} - \left[\begin{array}{c|c} \zeta[k_i+\Delta k_i] & 0\\ \hline 0 & 0\end{array}\right]\left\{\begin{array}{c} q_i\\ \hline u_b\end{array}\right\} = \left\{\begin{array}{c} 0\\ \hline F_b\end{array}\right\} \tag{27}$$

The last two terms on the left-hand side are added to the component representation inside of the mode projection multiplication, which is equivalent to adding Eq. (26) to the mode projection representation of Eq. (11). Equation (26) indicates the force response equilibrium between the component mode DOF denoted with ***i*** and boundary points denoted with *b*. However, the coefficient matrices in Eq. (27) lose their symmetry.

Symmetric Formulation of Modal Representation

To restore matrix symmetry, the vector transformation approach can be utilized.[16] Substituting Eq. (23) into Eq. (27), the further simplified form is obtained as

$$\left[\begin{array}{c|c} [I-\zeta]m_i & [I-\zeta]M_{ib}\\ \hline M_{ib}^T & M_{bb}\end{array}\right]s^2\left\{\begin{array}{c} q_i\\ \hline u_b\end{array}\right\} + \left[\begin{array}{c|c} k_i & 0\\ \hline 0 & K_{bb}\end{array}\right]\left\{\begin{array}{c} q_i\\ \hline u_b\end{array}\right\} = \left\{\begin{array}{c} 0\\ \hline F_b\end{array}\right\} \tag{28}$$

The diagonal matrix $[I-\zeta]^{-1/2}$ is premultiplied to the first row of Eq. (28). The mode shape at ***i*** points is linearly transformed in the following manner:

$$\sqrt{I-\zeta}\,\eta_i = q_i \tag{29}$$

Then, Eq. (24) becomes

$$\left[\begin{array}{c|c} [I-\zeta]^{\frac{1}{2}}m_i[I-\zeta]^{\frac{1}{2}} & [I-\zeta]^{\frac{1}{2}}M_{ib}\\ \hline M_{ib}^T[I-\zeta]^{\frac{1}{2}} & M_{bb}\end{array}\right]s^2\left\{\begin{array}{c} \eta_i\\ \hline u_b\end{array}\right\} + \left[\begin{array}{c|c} [I-\zeta]^{-\frac{1}{2}}k_i[I-\zeta]^{\frac{1}{2}} & 0\\ \hline 0 & K_{bb}\end{array}\right]\left\{\begin{array}{c} \eta_i\\ \hline u_b\end{array}\right\} = \left\{\begin{array}{c} 0\\ \hline F_b\end{array}\right\} \tag{30}$$

Because $[m_i]$, $[k_i]$, and $[I-\zeta]^{-1/2}$ are diagonal matrices, Eq. (30) can be redefined as

$$\left[\begin{array}{c|c} [I-\zeta]m_i & [I-\zeta]^{\frac{1}{2}}M_{ib}\\ \hline M_{ib}^T[I-\zeta]^{\frac{1}{2}} & M_{bb}\end{array}\right]s^2\left\{\begin{array}{c} \eta_i\\ \hline u_b\end{array}\right\} + \left[\begin{array}{c|c} k_i & 0\\ \hline 0 & K_{bb}\end{array}\right]\left\{\begin{array}{c} \eta_i\\ \hline u_b\end{array}\right\} = \left\{\begin{array}{c} 0\\ \hline F_b\end{array}\right\} \tag{31}$$

This algorithm does not change the stiffness of the component representation of the changed structure, even though the stiffness is changed in reality. If the mass matrix is also changed, according to Eq. (10) the changed mass matrix can be directly incorporated to Eq. (31). Furthermore, the damping change can be dealt with in this equation using the same approach as the mass matrix. Hence, the deviation of the original and changed mass matrix becomes

$$\Delta\tilde{M} = \Delta M + \left[\begin{array}{c|c} [I-\zeta]m_i & \sqrt{I-\zeta}M_{ib}\\ \hline M_{ib}^T\sqrt{I-\zeta} & M_{bb}\end{array}\right] - \left[\begin{array}{c|c} m_i & M_{ib}\\ \hline M_{ib}^T & M_{bb}\end{array}\right] = \Delta M + \left[\begin{array}{c|c} -\zeta m_i & \left[\sqrt{I-\zeta}-I\right]M_{ib}\\ \hline M_{ib}^T\left[\sqrt{I-\zeta}-I\right] & 0\end{array}\right] \tag{32}$$

The new modal responses of the original modal DOF after the change are obtained using this changed representation of the component.

System Equation and Its Characteristics

The effect of Eq. (26) is introduced in the equation of motion of the entire structure using the changed component representation of Eq. (32). The equation of motion of the entire structure after the change becomes

$$\left[m_j+\phi_j^T\Delta\tilde{M}\phi_j\right]s^2\{Q_j\} + \left[c_j+\phi_j^T\Delta C\phi_j\right]s\{Q_j\} + [k_j]\{Q_j\} = \{f_j\} \tag{33}$$

As compared with Eq. (12), the formulation developed here yields the modal mass-stiffness conversion in the component modes.

The reanalysis method in the frequency domain has already been proposed in Ref. 14 by the author. The final form of the equation, i.e., Eq. (33), yields the same representation in the previous work.[14] However, the derivation of the algorithm is totally different. Because the frequency-domain method in Ref. 14 employs the square of the frequency function, which cannot be defined in the time-response analysis, it may require a special transformation and assumptions. The equation derivation presented herein provides clear theoretical explanation of the time-domain reanalysis method compensating for the mode truncation effect.

Discussion on Numerical Application

Effect of Original Modes

The proposed method is characterized as a modified method of the mode projection with a mass-stiffness conversion, as shown in the comparison of Eqs. (12) and (33). Therefore, the change raised at the portion where the original mode shape does not have motion will not be incorporated in the system equation, which may produce a large computation error. However, because the equation of the component comprises generalized component modes, the component modes that have no response at the original analysis can be eliminated and interpreted as a change of the different modes that have responses at the original analysis. This can obviously be checked before reanalysis is performed.

Effect of Boundary Elements

Improvement by the proposed method is carried out only for component normal modes. The remaining issue is the effect of the change in the boundary matrices that are represented by ΔM_{bb} and ΔK_{bb}. These matrices are introduced in the system equation by the projection of the original global modes without the benefits of the proposed method. As the equation definition of the matrix, in the case of a single-point connection or having only rigid motion among the connection points between the component and the main structure, the stiffness matrix yields a zero matrix so that the truncation effect does not appear. A drastic change of motion between the connection points before and after the design change is not likely for real applications to the spacecraft–launch vehicle coupling problem because the launch vehicle is large and heavy enough. Therefore, the projection by the original global modes for the boundary matrices can adequately represent the force equilibrium.

Residual Flexibility and Matrix Condensation

Another concern is the comparison between the proposed method and the method with residual flexibility, if the flexibility matrix is

Table 1 Resonance frequencies

	Component		Entire structure[a]	
Mode no.	Frequency	Mode	Frequency	Mode
1	4.947	First bending *X* axis	0.0	Rigid
2	4.947	First bending *Y* axis	0.0	Rigid
3	29.08	Second bending *X* axis	0.0	Rigid
4	29.08	Second bending *Y* axis	0.0	Rigid
5	77	Third bending *X* axis	0.0	Rigid
6	77	Third bending *Y* axis	8.867	First bending *X* axis
7	134.2	Fourth bending *X* axis	8.867	First bending *Y* axis
8	134.2	Fourth bending *Y* axis	24.77	Second bending *X* axis
9	313	First axial	24.77	Second bending *Y* axis
10	891.4	Second axial	45.93	Third bending *X* axis
11	1334	Third axial	45.93	Third bending *Y* axis
12	1573	Fourth axial	75.53	Fourth bending *X* axis
13	——	——	75.53	Fourth bending *Y* axis

[a]Torsion motion is constrained.

available as a hypothetical case. Because the proposed method is based on the formulation of the residual flexibility shown in Eq. (8), comparable resulting accuracy can be expected if the model size is reduced by the transformation from Eq. (8) to Eq. (11) without any constraint for the equation of motion. However, if residual flexibility is available, it is possible to calculate using the size of matrix in Eq. (8), i.e., modal DOF and physical DOF of the changed component, which provides additional freedom to lead to further improvement against the error raised by the local force equilibrium. The Guyan reduction[17] is applied to Eq. (8); thus, Eq. (8) yields

$$[m_j]s^2\{Q_j\} + [c_j]s\{Q_j\} + \left[k_j + \phi_j^T Z\phi_j\right]\{Q_j\} + \left[\phi_j^T Z[Z+\Delta K]^{-1}\Delta M[Z+\Delta K]^{-1}Z\phi_j\right]s^2\{Q_j\} - \left[\phi_j^T Z[Z+\Delta K]^{-1}Z\phi_j\right]\{Q_j\} = \{f_i\} \tag{34}$$

For the stiffness matrix, the Guyan reduction yields the static condensation, which is rigorous condensation with no error. However, the Guyan reduction applied to the mass matrix is not perfect condensation. When substituting the stiffness change to the mass change according to the proposed method, Eq. (34) yields an equivalent equation form of Eq. (33) by introducing $\Delta K = 0$. This implies that the proposed method may impose an additional constraint on the method using the residual flexibility of Eq. (8), by reducing the matrix size into the modal DOF of Eq. (11) in the same manner using imperfect Guyan reduction for mass matrix. However, if relatively large numbers of DOFs are employed for the system equation due to providing sufficient freedom of motion, the accuracy deviation by the matrix size reduction into Eq. (11) will not be noticeable. The numerical comparison exhibiting this characteristic in the frequency-domain analysis was presented in Ref. 14.

Frequency-Domain Characteristics

Also, because Eq. (33) is equivalent to that of the frequency analysis in Ref. 14, the issues related to the magnitude of design variations and the influence on the modal frequency yield the same result as Ref. 14. Improvement from the conventional mode projection method in Eq. (12) is notable in large design change and at higher frequency modes, as shown in Ref. 14.

This method can be made available for general structural reanalysis problems other than spacecraft in a time domain, in which the structural component is subject to design changes. The reanalysis for a component on the large main structure driven by external force may be applied, i.e., aircraft components on the fuselage driven by engine thrust, or automobile components on the main body structure that is subjected to vibration from engine or wheels.

Examples

To estimate the ability of the proposed method, we present two examples: 1) a simplified numerical demonstration performed with a beam model and 2) a realistic application using a spacecraft–launch vehicle model.

Table 2 Excitation force function

$$F(t) = A_1\cos\omega_1 t + A_2\cos\omega_2 t$$
$$f_1 = \omega_1/2\pi = 8.0, \text{ Hz}$$
$$f_2 = \omega_2/2\pi = 20.0, \text{ Hz}$$
$$A_1 = A_2 = 1, \text{ N}$$

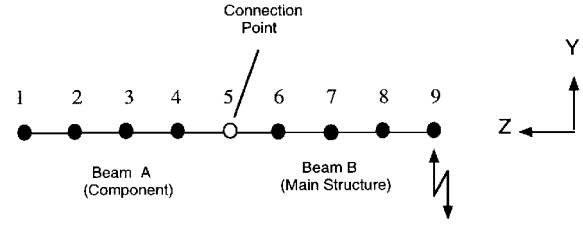

Fig. 1 Beam coupling model.

Simple Beam Model

The finite element computation, mode extraction, and equation transformation were performed using MSC/NASTRAN and its DMAP programming. All demonstrations were performed with the standard precision of MSC/NASTRAN. Two 25-DOF beams are employed to represent the changed component and the remaining unchanged parts of the structure, as shown in Fig. 1. Beam model A represents the spacecraft, and B represents launch vehicle. The coupled beam has the following dimension and properties: $EI = 560$ Nm, 900 mm in length, and 26.4 kg in total mass. An undamped condition is used for both the component and coupled structure. The coupled beam is subject to the excitation at tip point 9 of beam B. Both beams have homogeneous properties and the same grid point intervals. The dimension of this model causes little change in the mode shape at the excitation point before and after the design change shown on the right-hand side of Eq. (2). Nevertheless, as a typical application to verify the method's capability and adequacy, this simple symmetric component model configuration was chosen. The torsion DOFs are constrained to eliminate meaningless motion. The remaining three translation and two rotational DOFs are not constrained. Because the mass contribution for the rotational DOFs is not considered, 3 translation coordinates at 4 points yield a maximum of 12 elastic modes available for the component. In this demonstration, the full available 12 modes are used. The dynamic response is examined for the coupled structure. We assume beam A is modified to change its stiffness to double the original model. The excitation is assumed as a combination of two kinds of sinusoidal wave close to the resonance frequencies as a critical vibration. The resonance frequencies of the component and system equation of the entire structure and the excitation force function are presented in Tables 1 and 2, respectively. The resulting responses of the coupled model are shown in Fig. 2, in which five rigid modes and two elastic modes are employed for the system equation as the CLA result of

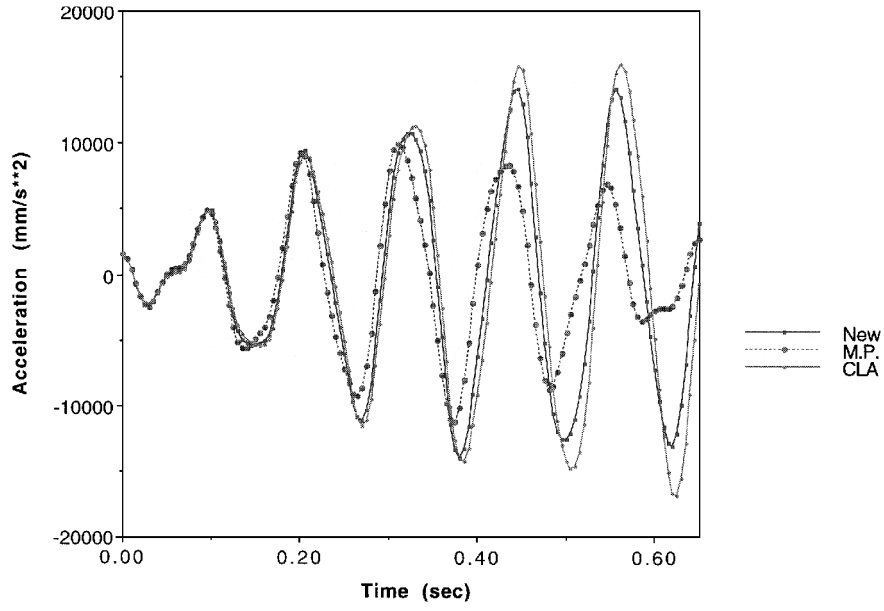

Fig. 2 Time response of beam model in two-elastic-mode case.

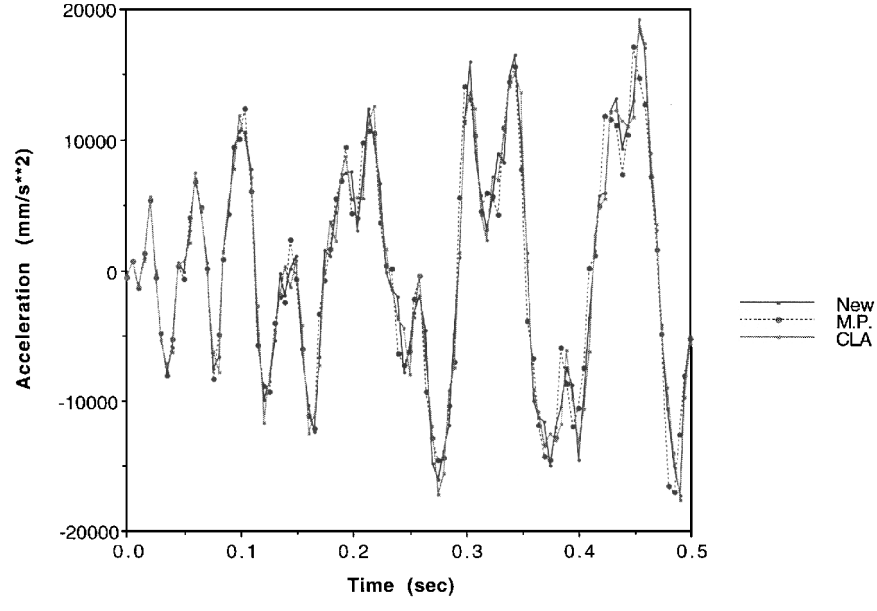

Fig. 3 Time response of beam model in eight-elastic-mode case.

the original structure. This is a typical case in that, in general, the CLA is performed using limited numbers of modal DOFs. As a comparison, the finite element (FE) analysis with full physical DOFs is conducted to demonstrate an additional standard CLA after change, which is indicated with the notation CLA in Fig. 2. The modal result of the former coupled analysis is the only information that is available for the reanalysis calculation after the design change. The straightforward approach is to use the projection of the changed physical characteristics by the original mode in the former CLA, which is presented in Eq. (12). The result, also illustrated in Fig. 2, is indicated with the notation of mode projection (M.P.). This method yields a poor result because of the effect of mode truncation, as shown in Fig. 2. The proposed method employs the same numbers of DOFs to the solution sequence as the mode projection method. Therefore, the improvement is accomplished by basically the same computation procedure with a few matrix manipulations added to the mode projection technique. The proposed method, indicated with a solid line, follows the exact response trajectory of the CLA, as shown in Fig. 2, where the proposed method is indicated with the notation of New. The slight deviation observed between the CLA and New may be caused by the effect of the matrix condensation discussed earlier.

The employment of five rigid and eight elastic modes for the response analysis is presented in Fig. 3. Because the improvement is provided by compensating the mode truncation, when employing sufficiently large numbers of modes the effect is diminished into a small difference in the response between the mode projection method and supplemental coupled load analysis starting from the physical matrix, as shown in Fig. 3. However, generally, the high possibility of mode truncation error is conceivable in large FE analysis because its flexibility is defined by a large number of DOFs.

Spacecraft–Launch Vehicle Model

As a realistic application, a reduced-matrix-size spacecraft and launch vehicle FE model is used, as shown in Fig. 4. This FE model is also constructed using MSC/NASTRAN with total 1362 DOFs including modal DOFs, referring to the published literature[18] and data from the real CLA results, as, for example, in Ref. 1. Although the real launch vehicle model is not available, even this reduced model can demonstrate the real result closely in terms of CLA. The stiffness and mass of the spacecraft are changed ranging between 0.5

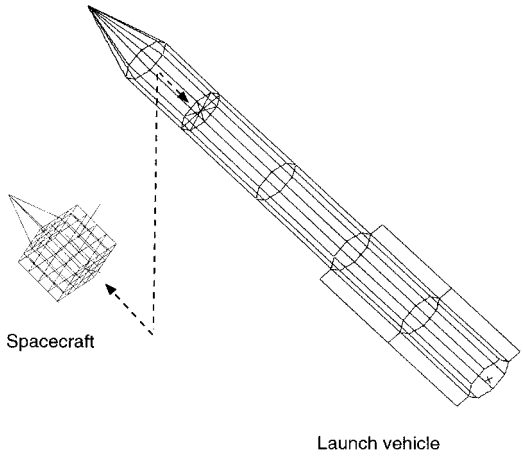

Fig. 4 Spacecraft–launch vehicle coupled model.

and 1.5 times. After eliminating uncoupled local modes, the lower 13 elastic modes are utilized for both the component modes and the coupled system analysis in which 5 modes for the coupled system are rigid modes. The natural frequency of the spacecraft component modes before and after the structural changes are presented in Table 3. Solving the coupling model, the frequency changes of the entire structure caused by the design change in the spacecraft are presented in Table 4 to clarify the condition of the demonstration. In this demonstration, a shock excitation is applied to the tail end of the launch vehicle, which simulates the main engine cutoff or the ignition delay of solid boosters of the launch vehicle. The time response by the mode projection method, the proposed method, and the supplemental CLA after changes are compared. The proposed method can provide good coherence with the result of the additional CLA conducted with the entire DOFs associated with the changed component. The results are presented in Figs. 5 and 6, which illustrate time responses at a typical point on the spacecraft in terms of two directions: the shock excitation direction on the launch vehicle and normal to it.

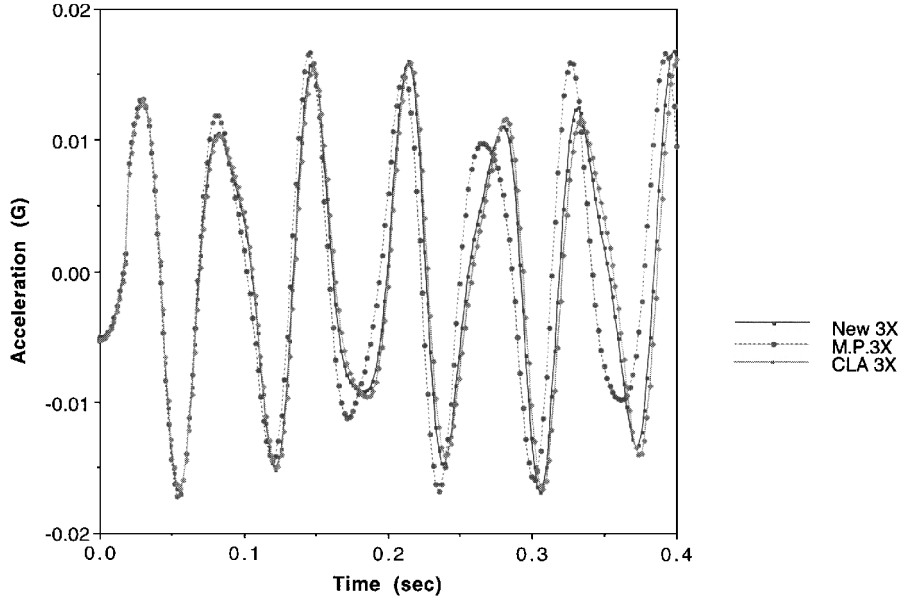

Fig. 5 Time response of spacecraft–launch vehicle coupling model, *X* axis.

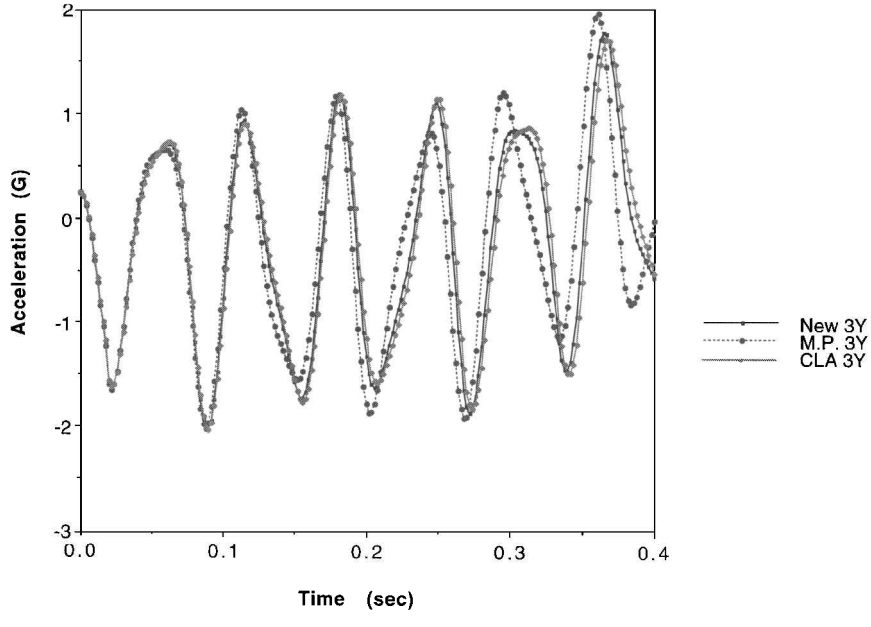

Fig. 6 Time response of spacecraft–launch vehicle coupling model, *Y* axis.

Table 3 Component resonance frequencies

Mode no.	Frequency	
	Before change	After change
1	3.137	2.020
2	4.040	4.706
3	7.921	9.390
4	18.78	11.68
5	22.98	11.88
6	23.36	18.29
7	28.22	26.82
8	36.58	29.11
9	39.08	32.00
10	53.64	34.47
11	59.87	42.34
12	62.07	58.62
13	64.01	93.11

Table 4 Resonance frequencies of entire structure

Mode no.	Frequency	
	Before change	After change
1–5[a]	0.0	0.0
6	1.726	1.641
7	1.788	1.815
8	5.385	5.818
9	12.53	11.31
10	20.16	15.93
11	21.87	16.14
12	23.22	26.90
13	24.99	27.68

[a]Torsion motion is constrained.

Conclusion

An analytical verification method is proposed of structural dynamics after a design change with the aim of enhancing the reliability and flexibility of the structural design methodology applied to the design change procedure. With the proposed method, repetitive tests and eigenanalyses of the entire structure including the unchanged portion are not required. Only a small number of modal parameters from the time-domain force response analysis with the original structure and the changed physical property information are required, so that the design change can be incorporated with minimum impact on schedule at any time. The feature of the mathematical formulation based on the mode acceleration technique can provide an easy computational scheme and accurate results. The examples presented show the effectiveness of the proposed method. When applying the method to spacecraft–launch vehicle coupled load analysis, the physical characteristic information of the launch vehicle and repetition of eigenanalysis are not required, even though the established algorithm is derived from the coupled spacecraft and launch vehicle structural characteristics.

Acknowledgments

This study was performed as part of the research and development project of the Nippon Telegraph and Telephone Corporation telecommunications satellite. The author would like to thank the staff of the ETS-VI and N-STAR satellite projects for their cooperation.

References

[1]Hamilton, D. A., "A Review of Shuttle Payload Bay Low-Frequency Response for STS-1 Though STS-5," AIAA Paper 83-2579, Oct. 1983.

[2]Stetson, K. A., "Perturbation Method of Structural Design Relevant to Holographic Vibration Analysis," *AIAA Journal*, Vol. 13, No. 4, 1975, pp. 457–459.

[3]Baldwin, J. F., and Hutton, S. G., "Natural Modes of Modified Structures," *AIAA Journal*, Vol. 23, No. 11, 1985, pp. 1737–1743.

[4]Wang, B. P., and Pilkey, W. D., "Eigenvalue Reanalysis of Locally Modified Structures Using a Generalized Rayleigh's Method," *AIAA Journal*, Vol. 24, No. 6, 1986, pp. 983–990.

[5]Bernitsas, M. M., and Kang, B., "Admissible Large Perturbation in Structural Redesign," *AIAA Journal*, Vol. 29, No. 1, 1991, pp. 104–113.

[6]Coppolino, R. N., "Structural Mode Sensitivity to Local Modification," Society of Automotive Engineers, SAE Paper 811044, Oct. 1981.

[7]Engels, R. C., Craig, R. R., Jr., and Harcrow, H. W., "A Survey of Payload Integration Methods," *Journal of Spacecraft and Rockets*, Vol. 21, No. 5, 1984, pp. 417–424.

[8]Craig, R. R., and Bampton, M. C., "Coupling of Substructures for Dynamic Analysis," *AIAA Journal*, Vol. 6, No. 8, 1968, pp. 1313–1319.

[9]Benfield, W. A., and Hruda, R. F., "Vibration Analysis of Structures by Component Mode Substitution," *AIAA Journal*, Vol. 9, No. 7, 1971, pp. 1255–1261.

[10]"MSC/NASTRAN Theoretical Manual," MSC Corp., 9.4.-1, Los Angeles, CA, Dec. 1972.

[11]Yasui, Y., "Decomposition Method for Mode Shape Identification Using Measured Data," *Japan Society of Mechanical Engineering International Journal III*, Vol. 35, No. 2, 1992, pp. 279–285.

[12]Karpel, H., and Raveh, D., "Fictitious Mass Element in Structural Dynamics," *AIAA Journal*, Vol. 34, No. 3, 1996, pp. 607–613.

[13]Spanos, P. D., and Majed, A., "A Residual Flexibility Approach for Decoupled Analysis of Systems of Combined Components," *Journal of Vibration and Acoustics*, Vol. 118, Oct. 1996, pp. 682–686.

[14]Yasui, Y., "Improved Mode Superposition Reanalysis Method," *Computers and Structures*, Vol. 48, No. 4, 1993, pp. 711–717.

[15]Jezequel, L., "Procedure to Reduce the Effects of Modal Truncation in Eigensolution Reanalysis," *AIAA Journal*, Vol. 28, No. 5, 1990, pp. 896–902.

[16]MacNeal, R. H., Citerley, R., and Chargin, M., "A Symmetric Modal Formulation of Fluid–Structure Interaction, Including a Static Approximation to Higher Order Fluid Modes," American Society of Mechanical Engineers, ASME Paper 80-C2/PVP-116, Aug. 1981.

[17]Guyan, R. J., "Reduction of Stiffness and Mass Matrices," *AIAA Journal*, Vol. 3, No. 2, 1965, p. 380.

[18]NASDA, "H-II Launch Vehicle User's Manual," NASDA-HDBK-1002 Notice1, National Space Development Agency, Tokyo, Japan, Oct. 1996.

A. Berman
Associate Editor